Cooperative Effect of Electron Correlation and Spin-Orbit Coupling on the Electronic and Magnetic Properties of Ba_2NaOsO_6

H. J. Xiang and M.-H. Whangbo*
Department of Chemistry, North Carolina State University, Raleigh, North Carolina 27695-8204
(Dated: February 4, 2008)

The electronic and magnetic properties of the cubic double perovskite Ba_2NaOsO_6 were examined by performing first-principles density functional theory calculations and analyzing spin-orbit coupled states of an Os^{7+} (d^1) ion at an octahedral crystal field. The insulating behavior of Ba_2NaOsO_6 was shown to originate from a cooperative effect of electron correlation and spin-orbit coupling. This cooperative effect is responsible not only for the absence of orbital ordering in Ba_2NaOsO_6 but also for a small magnetic moment and a weak magnetic anisotropy in Ba_2NaOsO_6.

PACS numbers: 71.70.Ej, 71.27.+a, 71.20.-b, 75.30.Gw

Oxides of orbitally degenerate 3d transition metal ions at octahedral sites exhibit rich electronic and magnetic properties arising from the interplay between spin, orbital and charge degrees of freedom. In an octahedral crystal field, the d-orbitals of a transition metal ion are split into the t_{2g} and e_g levels. A 3d perovskite with unevenly filled e_g levels, e.g., $LaMnO_3$ with high-spin Mn^{3+} ($3d^4$) ions, has a strong tendency for orbital ordering [1]. In contrast, a 3d perovskite with unevenly filled t_{2g} levels, e.g., $YTiO_3$ with Ti^{3+} ($3d^1$) ions, has a reduced tendency for orbital ordering and hence provides opportunities to observe an intricate interplay between the spin and orbital dynamics [2, 3]. It is an important issue to understand the mechanisms that select the ground state out of numerous possible states arising from this competition [2, 3, 4, 5].

Most studies probing this question have focused on 3d oxides, and much less is known about whether related 4d and 5d oxides can exhibit similar behavior. Due to a large spatial extension of 5d orbitals, effects of electron-correlation are weaker in 5d oxides than in 3d oxides. However, effects of spin-orbit coupling (SOC) are stronger in 5d oxides than in 3d oxides. Thus, 5d oxides should exhibit a different balance between spin, orbital and charge degrees of freedom. In this context, it is of interest to examine the electrical and magnetic properties of the cubic double perovskite Ba_2NaOsO_6 [6, 7, 8]. In this 5d oxide the NaO_6 octahedra share corners with the OsO_6 octahedra of orbitally degenerate Os^{7+} ($5d^1$) ions, and the nearest-neighbor OsO_6 octahedra run along the [110] direction while the next-nearest-neighbor OsO_6 octahedra run along the [100] direction (Figure 1). Ba_2NaOsO_6 presents several puzzling properties. It is an insulator despite the fact that the structure remains cubic down to 5 K without any distortion of the OsO_6 octahedra from their regular octahedral shape [8]. It is unclear what mechanism lifts the orbital degeneracy of the Os^{7+} (d^1) ions to make Ba_2NaOsO_6 insulating. The magnetic susceptibility of Ba_2NaOsO_6 between 75 and 200 K follows a Curie-Weiss law with a negative Weiss temperature (i.e. $\theta \approx -10$ K), which shows that the dominant spin exchange interaction between Os^{7+} ions is antiferromagnetic (AFM) [7, 8]. However, Ba_2NaOsO_6 undergoes a ferromagnetic (FM) ordering below $T_C = 6.8$ K with a very low magnetic moment, i.e., $\sim 0.2\ \mu_B$ per formula unit (FU) [7, 8].

TABLE I: Comparison of the zero-field magnetic moments μ_{exp} (per FU) with the calculated moments μ_{calc} (per FU) for the ferromagnetic state of Ba_2NaOsO_6 using the GGA+SOC+U method with $U_{eff} = 0.2$ Ryd [a,b].

	μ_S(Os)	μ_L(Os)	μ_S	μ_{calc}	μ_{exp} [c]
[111]	0.51	-0.35	0.98	0.63	0.19
[110]	0.51	-0.34	0.98	0.64	0.22
[100]	0.52	-0.30	0.97	0.67	0.18

[a] μ_S(Os) and μ_L(Os) are the spin and orbital magnetic moments calculated for the Os atom, respectively, and μ_S is the calculated total spin magnetic moment per FU.
[b] The moments are in units of μ_B.
[c] Ref. [8]

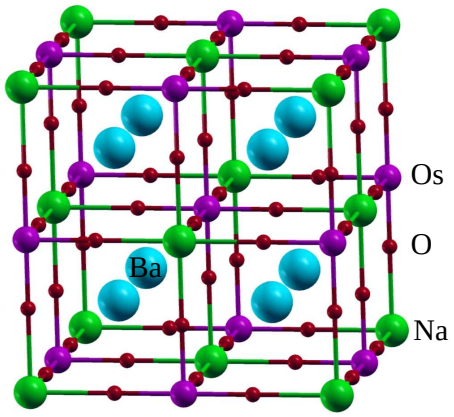

FIG. 1: (Color online) Structure of cubic double perovskite Ba_2NaOsO_6.

To gain insight into the puzzling electronic and magnetic properties of Ba_2NaOsO_6, we carried out a first-

principles density functional theory (DFT) electronic structure study. In this Letter, we show that the insulating property of Ba_2NaOsO_6 originates from a cooperative effect of electron correlation and SOC. This cooperative effect is responsible not only for the lack of structural distortion in Ba_2NaOsO_6 but also for the low magnetic moment and the weak magnetic anisotropy [8] of Ba_2NaOsO_6 in the FM state.

Our first principles DFT electronic structure calculations were performed by using the full-potential augmented plane waves plus local orbital method as implemented in the WIEN2k code [9]. The non-overlapping muffin-tin sphere radii of 2.50, 2.14, 1.86, and 1.65 au are used for the Ba, Na, Os and O atoms, respectively. The expansion in spherical harmonics of the radial wave functions were taken up to $l = 10$. The value of $R_{MT}^{min}K_{max}$ was set to 7.0. The total Brillouin zone was sampled with 125 k-points. For the exchange-correlation energy functional, the generalized gradient approximation (GGA) by Perdew, Burke and Ernzerhof [10] was employed. The SOC was included on the basis of the second-variational method using scalar relativistic wave functions [11]. The structural parameters of Ba_2NaOsO_6 were taken from the experimental values [7].

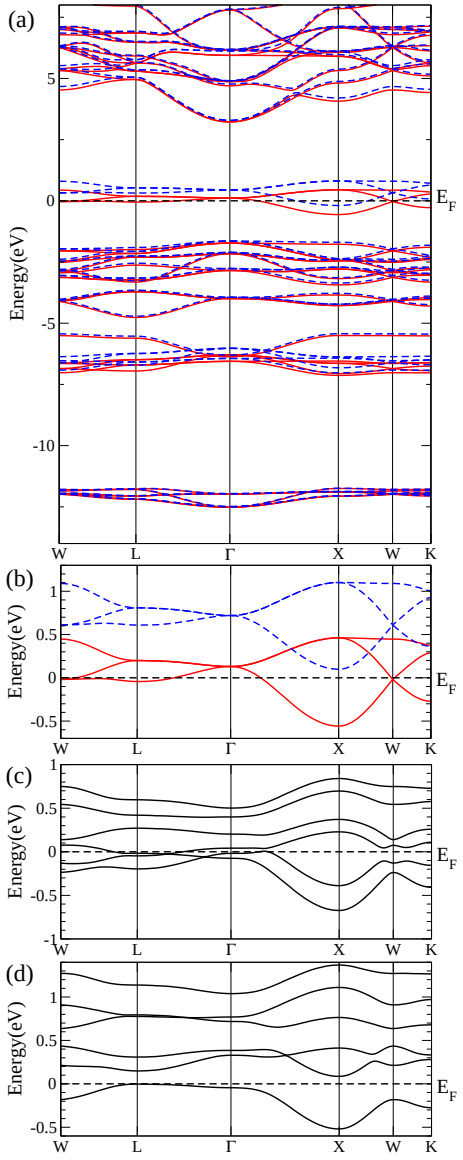

FIG. 2: (Color online) Band structures calculated for Ba_2NaOsO_6 using different methods. (a) GGA, (b) GGA+U with $U_{eff} = 0.2$ Ryd, (c) GGA+SOC, (d) GGA+SOC+U with $U_{eff} = 0.2$ Ryd. In (a) and (b) the solid and dashed lines refer to the up- and down spin bands, respectively. In (d) the valence band top is taken as the zero-energy point.

The spin-polarized GGA band structure calculated for the FM state of Ba_2NaOsO_6, presented in Figure 2(a), has the Fermi level crossing both the up- and down-spin t_{2g} bands. This does not agree with the fact that Ba_2NaOsO_6 is an insulator [8]. At Γ the three t_{2g} bands are degenerate. The overall width of the t_{2g} bands is narrow (approximately 1 eV) because the nearest-neighbor O$\cdots$O distance between adjacent OsO_6 octahedra is long (3.216 Å) compared with the van der Waals distance of 3.04 Å. The exchange splitting of Ba_2NaOsO_6 is about 0.34 eV, which is considerably smaller than typical values found for 3d magnetic oxides. Because the bandwidth is small compared with the on-site repulsion U (approximately 3.3 eV), it was suggested [8] that electron correlation is important in Ba_2NaOsO_6. The failure of the traditional DFT in describing strongly correlated systems is currently remedied by the DFT plus on-site repulsion U method [12, 13, 14]. Thus, we employed the GGA+U method to see if the insulating property of Ba_2NaOsO_6 can be explained. To avoid a double counting in the non-spherical part of potential, we used $U_{eff} = U - J$ and omit the multipolar terms proportional to J in the added GGA+U potential. The band structure calculated for

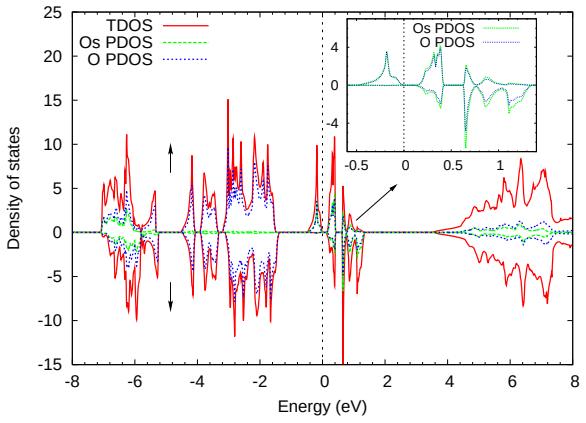

FIG. 3: (Color online) DOS of Ba_2NaOsO_6 obtained from the GGA+SOC+U calculation. The inset shows the PDOS plots calculated for the Os and O atom contributions to the t_{2g} bands.

the FM state of Ba_2NaOsO_6 using the GGA+U method with $U_{eff} = 0.2$ Ryd is shown in Figure 2(b), which reveals a larger exchange splitting (about 0.7 eV). However, there is no band splitting at Γ, and the dispersion characteristics of the t_{2g} bands are almost the same as those of the GGA calculation. Our GGA+U calculations with larger U_{eff} values (up to 0.5 Ryd) did not change the general picture described above. Since Os is a heavy element, SOC is expected to play an important role in Ba_2NaOsO_6. To see the effect of SOC on the electronic structure of Ba_2NaOsO_6, we performed GGA+SOC calculations. Figure 2(c) shows the band structure calculated for the FM state using the GGA+SOC method with the spin quantization taken along the [111] direction. The up- and down-spin t_{2g} bands are both split into three non-degenerate bands at Γ. However, these bands overlap with each other leading to a metallic state for Ba_2NaOsO_6.

As described above, the GGA, GGA+U, and GGA+SOC methods all fail to reproduce the insulating state for Ba_2NaOsO_6. Nevertheless, we note that electron correlation enhances the exchange splitting, while SOC splits the t_{2g} bands. This suggests that a combined effect of electron correlation and SOC might induce a band gap in both the up- and down-spin t_{2g} bands. Therefore, we carried out GGA+SOC+U calculations for Ba_2NaOsO_6. The band structure calculated for the FM state with the spin quantization along the [111] direction is presented in Figure 2(d), which shows that Ba_2NaOsO_6 has an insulating gap with the lowest-lying down-spin t_{2g} band lying above the Fermi level. The associated density of states (DOS) calculated for Ba_2NaOsO_6 is shown in Figure 3. The partial DOS (PDOS) plots for the Os 5d and O 2p states reveal that the Os 5d and the O 2p states contribute almost equally in the t_{2g} bands. Though not shown, the PDOS plots calculated for the Os $5d_{xz}$, $5d_{yz}$ and $5d_{xy}$ orbitals show that these orbitals contribute equally to the t_{2g} bands. The Os-O bonding bands of the e_g-symmetry occur well below the Fermi level (i.e., in the energy region between −7 and −5 eV), which indicates the presence of a strong covalent bonding in the Os-O bonds.

So far, our calculations were performed for the FM state of Ba_2NaOsO_6. To find if the FM state is the magnetic ground state, we considered an A-type AFM state in which the spins have the FM ordering within each sheet of Os^{7+} ions parallel to the (001) plane, but have the AFM ordering between adjacent sheets parallel to the (001) plane. Our GGA+SOC+U calculation shows that the A-type AFM state is considerably less stable than the FM state (by 267 meV/FU), which is consistent with the observation that Ba_2NaOsO_6 undergoes an FM ordering below 6.8 K [8]. In the remainder of this work we will consider only the electronic structures calculated for the FM state of Ba_2NaOsO_6.

To examine the effect of the spin quantization direction on electronic structure, we carried out GGA+SOC and GGA+SOC+U calculations for the FM state of Ba_2NaOsO_6 with the spin quantization taken along the [111], [110] and [100] directions. The stability dependence of the FM state on the spin quantization direction is negligible in the GGA+SOC calculations, but is not negligible in the GGA+SOC+U calculations. In the latter calculations with $U_{eff} = 0.2$ Ryd, the FM states with the [110] and [100] quantizations are less stable than that with the [111] quantization by 1.9 and 16 meV per FU, respectively. The spin, orbital and total moments calculated for the FM state of Ba_2NaOsO_6 using the GGA+SOC+U method with $U_{eff} = 0.2$ Ryd are summarized in Table I. For each of the [111], [110] and [100] quantizations, the total moment per FU is calculated to be $\sim 0.65\mu_B$, which is smaller than the spin-only value of 1 μ_B due to the fact that the orbital moment of $\sim 0.33\mu_B$ is opposite to the spin moment in direction. Nevertheless, the calculated values are still large compared with the zero-field moments ($\sim 0.2\mu_B$/FU) determined from the magnetization study of Ba_2NaOsO_6 [7, 8].

The band gap opening at the Fermi level, the moment reduction and the slight magnetocrystalline anisotropy in Ba_2NaOsO_6 can be accounted for by considering the effect of SOC on the t_{2g} orbitals of an Os^{7+} ion. In the second variational approach for spin-orbit coupling [11], the scalar-relativistic part of the Hamiltonian is diagonalized on a basis adopted for each of the spin projections separately, and then the full Hamiltonian matrix is constructed on the basis of the eigenfunctions obtained in the first step. The spin-orbit part of the Hamiltonian in the Os spheres is then given by

$$\hat{H}_{so} = \lambda \hat{\mathbf{L}} \cdot \hat{\mathbf{S}}, \tag{1}$$

where the SOC constant $\lambda > 0$ for the Os^{7+} (d^1) ion with less than half-filled t_{2g} levels. With θ and ϕ as the azimuthal and polar angles of the magnetization in the rectangular crystal coordinate system, the $\hat{\mathbf{L}} \cdot \hat{\mathbf{S}}$ term is rewritten as

$$\begin{aligned} \hat{\mathbf{L}} \cdot \hat{\mathbf{S}} \;=\; & \hat{S}_z(\hat{L}_z \cos\theta + \tfrac{1}{2}\hat{L}_+ e^{-i\phi}\sin\theta + \tfrac{1}{2}\hat{L}_- e^{i\phi}\sin\theta) \\ & + \tfrac{1}{2}\hat{S}_+(-\hat{L}_z \sin\theta - \hat{L}_+ e^{-i\phi}\sin^2\tfrac{\theta}{2} + \hat{L}_- e^{i\phi}\cos^2\tfrac{\theta}{2}) \\ & + \tfrac{1}{2}\hat{S}_-(-\hat{L}_z \sin\theta - \hat{L}_+ e^{-i\phi}\cos^2\tfrac{\theta}{2} + \hat{L}_- e^{i\phi}\sin^2\tfrac{\theta}{2}). \end{aligned} \tag{2}$$

Since the up- and down-spin t_{2g} bands are separated due to the exchange splitting, one can neglect interactions between the up- and down-spin states under the SOC to a first order approximation. This allows one to consider only the up-spin t_{2g} bands using the degenerate perturbation theory, which requires the construction of the matrix elements $\langle i|\hat{H}_{so}|j\rangle$ $(i, j = d_{xy}, d_{yz}, d_{xz})$ [15]. In this case, only the operators of the first line of Eq. 2 give rise to nonzero matrix elements. In evaluating these matrix elements, it is convenient to rewrite the angular parts of the d_{xy}, d_{yz} and d_{xz} orbitals in terms of the spherical

harmonics as

$$\begin{aligned} d_{xy} &= \tfrac{-i}{\sqrt{2}}(Y_2^2 - Y_2^{-2}) \\ d_{yz} &= \tfrac{i}{\sqrt{2}}(Y_2^1 + Y_2^{-1}) \\ d_{xz} &= \tfrac{-1}{\sqrt{2}}(Y_2^1 - Y_2^{-1}). \end{aligned} \quad (3)$$

Using these functions, the matrix representation $\langle i|\hat{H}_{so}|j\rangle$ is found as

$$i\hbar\lambda/2 \begin{pmatrix} 0 & \sin\theta\sin\phi & -\sin\theta\cos\phi \\ -\sin\theta\sin\phi & 0 & \cos\theta \\ \sin\theta\cos\phi & -\cos\theta & 0 \end{pmatrix}. \quad (4)$$

Upon diagonalizing this matrix, we obtain the eigenvalues of the three spin-orbit coupled states, namely, $E_1 = -\hbar\lambda/2$, $E_2 = 0$, $E_3 = \hbar\lambda/2$. The associated eigenfunctions Ψ_1, Ψ_2, Ψ_3 are given by

$$\begin{aligned} \Psi_1 &= \tfrac{\sqrt{2}}{2}[\sin\theta d_{xy} + (i\sin\phi - \cos\theta\cos\phi)d_{yz} \\ &\quad -(i\cos\phi + \cos\theta\sin\phi)d_{xz}] \\ \Psi_2 &= \tfrac{\sqrt{2}}{2}[\sin\theta d_{xy} - (i\sin\phi + \cos\theta\cos\phi)d_{yz} \\ &\quad +(i\cos\phi - \cos\theta\sin\phi)d_{xz}] \\ \Psi_3 &= \cos\theta d_{xy} + \sin\theta\cos\phi d_{yz} + \sin\theta\sin\phi d_{xz}. \end{aligned} \quad (5)$$

For these three states Ψ_1, Ψ_2, and Ψ_3, the orbital moments L along the spin quantization direction are $-1\mu_B$, 0 and $1\mu_B$, respectively, according to their eigenvalues and the SOC operator $\hat{H}_{so} = \lambda\hat{\mathbf{L}}\cdot\hat{\mathbf{S}}$ given that S = 1/2. Since the spin-orbit coupled state Ψ_1 is occupied, we obtain a negative orbital moment. The moment of $-0.35\mu_B$ from the GGA+SOC+U calculation is considerably smaller in magnitude than $-1\mu_B$. This is not surprising because the above analysis neglected the fact that the t_{2g} orbitals of an OsO_6 octahedron are not pure $5d_{xz}$, $5d_{yz}$ and $5d_{xy}$ orbitals of the Os atom, but are given by their linear combinations with the 2p orbitals of the surrounding O atoms. Given that the Os 5d and the O 2p states contribute almost equally in the t_{2g} bands (Figure 3), an orbital moment of approximately $-0.5\mu_B$ should be expected from the occupation of the up-spin t_{2g} band associated with Ψ_1.

The above analysis indicates that SOC splits the t_{2g} bands into three subbands regardless of the direction of the magnetization. However, SOC does not affect the exchange splitting. It is the on-site repulsion that enhances the exchange splitting and increases the energy separation between filled and empty bands within each spin channel. That is, a cooperative effect of electron correlation and SOC is essential in opening a band gap at the Fermi level for Ba_2NaOsO_6. Eq. 5 shows that the contributions of the d_{xy}, d_{yz} and d_{xz} orbitals to the spin-orbit coupled state Ψ_1 depend on the direction of the magnetization (i.e., $\theta = 90°$ and $\phi = 0°$ for [100]; $\theta = 90°$ and $\phi = 45°$ for [110]; $\theta = \arccos(\sqrt{3}/3)$ and $\phi = 45°$ for [111]). This is responsible for the weak magnetic anisotropy observed for Ba_2NaOsO_6 [8]. The three d-orbitals contribute equally to the state Ψ_1 for the [111] spin quantization, but unequally for the [110] and [100] spin quantizations. The inter-octahedron hopping integral is nonzero along the directions of nearest-neighbor OsO_6 octahedra (e.g., [111] and [110]) but is practically zero along the directions of next-nearest-neighbor OsO_6 octahedra (e.g., [100]). For the [100] spin quantization, the Ψ_1 level does not provide hopping along the [011] direction because it has no d_{yz} orbital contribution. Consequently, the spin-orbit coupled band associated with Ψ_1 should be higher in energy for the [100] quantization than for the [111] and [110] quantizations. This in part explains why the [100] quantization leads to a higher electronic energy than do the [111] and [110] quantizations.

In summary, the insulating behavior of Ba_2NaOsO_6 is caused by a novel cooperative effect of electron correlation and SOC, which opens a band gap at the Fermi level and hence removes a driving force for orbital ordering of the orbitally degenerate $Os^{7+}(d^1)$ ions. The small magnetic moment of Ba_2NaOsO_6 arises from the fact that the occupied spin-orbit-coupled up-spin t_{2g} band gives rise to an orbital moment that is in opposite direction to the spin moment.

The research was supported by the Office of Basic Energy Sciences, Division of Materials Sciences, U. S. Department of Energy, under Grant No. DE-FG02-86ER45259.

* Corresponding author. E-mail: mike_whangbo@ncsu.edu

[1] W.-G. Yin *et al.*, Phys. Rev. Lett. **96**, 116405 (2006).
[2] C. Ulrich *et al.*, Phys. Rev. Lett. **89**, 167202 (2002).
[3] R. Schmitz *et al.*, Ann. Phys. **14**, 626 (2005).
[4] G. Khaliullin and S. Okamoto, Phys. Rev. Lett. **89**, 167201 (2002).
[5] E. Pavarini *et al.*, Phys. Rev. Lett. **92**, 176403 (2004).
[6] A. W. Sleight *et al.*, Inorg. Chem. **1**, 245 (1962).
[7] K. E. Stitzer *et al.*, Solid State Sci. **4**, 311 (2002).
[8] A. S. Erickson *et al.*, cond-mat/0610385.
[9] P. Blaha *et al.*, in WIEN2K, An Augmented Plane Wave Plus Local Orbitals Program for Calculating Crystal Properties, edited by K. Schwarz (Techn. Universität Wien, Austria, 2001).
[10] J. P. Perdew *et al.*, Phys. Rev. Lett. **77**, 3865 (1996).
[11] J. Kuneš *et al.*, Phys. Rev. B **63**, 205111 (2001) and references therein.
[12] V. I. Anisimov *et al.*, Phys. Rev. B **48**, 16929 (1993).
[13] Our calculations using the method of Czyzyk and Sawatzky led essentially to the same results. See: M. T. Czyzyk and G. A. Sawatzky, Phys. Rev. B **49**, 14211 (1994).
[14] Our calculations using the local density approximation led essentially to the same results except that a larger U_{eff} (> 0.21 Ryd) is needed to open an insulating gap.
[15] D. Dai and M.-H. Whangbo, Inorg. Chem. **44**, 4407 (2005).